ELSEVIER

Ultramicroscopy 65 (1996) 147–158

ultramicroscopy

Method for controlled formation of vitrified films for cryo-electron microscopy

Nikolai D. Denkov *, Hideyuki Yoshimura [1], Kuniaki Nagayama [2]

Protein Array Project, ERATO, JRDC, Tsukuba Research Consortium, 5-9-1 Tokodai, Tsukuba 300-26, Japan

Received 17 May 1996; revised 22 July 1996; accepted 20 August 1996

Abstract

A novel method for controlled formation of large, unsupported vitrified films for cryo-electron microscopy is described. Liquid films of diameter between 40 and 150 μm are formed in the central hole of a thin, disc-shaped specimen holder. The bulk liquid, surrounding the film, is connected through a glass capillary to a microsyringe, which allows the fine control of the film radius. The processes of liquid film formation and subsequent thinning are observed in reflected, monochromatic light by means of a CCD-camera equipped with a long-focus magnifying lens. The film thickness is precisely determined from the intensity of light, reflected from the film. In this way the vitrification can be accomplished at desired film thickness and radius. The control of the liquid film radius and thickness is utilized to produce well ordered two-dimensional arrays of monodisperse particles (latex spheres and protein/lipid vesicles) just before the film freezing, without need of specific binding agents. At suitable conditions ordered bilayers and triple-layers of particles are obtained.

1. Introduction

Cryo-electron microscopy of thin vitrified films offers the unique possibility for a high resolution structural analysis of biosamples that are not suitable for direct X-ray or NMR investigation [1,2]. Vitrification ensures excellent structure preservation of hydrated molecules and biomolecular complexes [3,4]. The vitrified samples do not need staining and fixation reagents which could affect the molecular structure and reduce the resolution. In addition, the radiation damage, caused by the electron beam, is decreased several times due to the low working temperature [5–7]. Cryo-microscopy has yielded valuable structural information for viruses [8–12], membrane proteins [13–17], and protein complexes [4,18–22]. The method is of particular use for visualisation of soft, unstable when dried molecular aggregates, like lipid vesicles [23–27], microemulsions [28], and surfactant micelles [29–33].

Two procedures for preparation of vitrified films for cryo-electron microscopy are widely used. In the first, the film is spread on a hydrophilic carbon layer deposited on an electron microscope grid [1,13,34].

* Corresponding author. Permanent address: Laboratory of Thermodynamics and Physico-chemical Hydrodynamics, Faculty of Chemistry, Sofia University, 1 "James Bouchier" Avenue, 1126 Sofia, Bulgaria. Fax: +359 2 9625643; E-mail: Denkov@Ltph.cit.bg.

[1] Present address: Department of Physics, School of Science and Technology, Meiji University, 1-1-1 Higashimita, Tama-ku, Kawasaki 214, Japan. Fax: +89 44 900 0421; E-mail: hyoshi@isc.meiji.ac.jp.

[2] Present address: Department of Life Sciences, The University of Tokyo, Komaba, Meguro, Tokyo 153, Japan. Fax: +81 3 5454 4332; E-mail: nagayama@orca.c.u-tokyo.ac.jp.

PII S0304-3991(96)00065-4

In the second, the films are formed without any support in the holes of the grid (so called "bare grid method" [8]). Several others, more complex procedures for film formation, were also tested – see e.g. the discussion in Ref. [1]. One particular feature of these methods is that liquid films of micrometer diameter are used, which precludes direct optical observation and control of the film formation and thinning processes. In a recent study Jakubowski and Mende [35] tried to vitrify larger in diameter unsupported films (more than 50 μm in diameter) stabilised by lipid. The results of their experiments were not very encouraging, however – the authors concluded that "ultrathin non-collapsed water films can be cryofixed only occasionally" [35].

The major aim of our study is to develop a method for controlled formation of large, unsupported vitrified films, whose thickness is precisely measured by direct video-microscopic observation. We found that at appropriate conditions films of diameter between 40 and 150 μm can be reproducibly vitrified if their thickness is around (or above) 50 nm. In several cases we vitrified films of thickness around 30 nm. The control over the film radius and thickness offers new prospects for research and some of them are discussed below. Some of the results, obtained by our method, have been reported already (without technical details) as a brief Letter [36]. The present article is mostly oriented to describe the practical procedures for film formation, observation, control, and vitrification.

2. Description of the method

2.1. Experimental set-up, film formation and control of the film radius

The film is formed from a liquid drop, placed in the central hole of a disc-shaped copper holder (60 μm thick, 3 mm in diameter), which is produced by standard etching procedure (special order to Oyourika Co., Tokyo, Japan) – see Fig. 1. The central hole (400 μm in diameter) is connected by a 50 μm wide slit (channel) with the periphery of the holder. During the film formation and subsequent thinning a narrow glass capillary is touching the outer end of the channel. The capillary is connected to a microsyringe to allow for the accurate suction or ejection of liquid. In this way the volume of liquid suspended in the holder is precisely controlled. After suction of a certain amount of liquid from the drop, a planar film of homogeneous thickness is formed in the center of the hole – Fig. 2. The film is surrounded by a thicker, biconcave liquid layer (meniscus region). The film radius (typically between 20 and 80 μm) can be increased/decreased by suction/extrusion of minute amounts of liquid through the capillary. When observed in reflected monochromatic light, the planar film is seen as a homogeneous circular area whose brightness strongly depends on the film thickness (Fig. 2). The surrounding meniscus appears as a dark ring. For observation and subsequent film thickness determination (see below) we used a CCD-camera (XC-77, Sony) equipped with a magnifying long-focus lens (CTL-6, Tokyo Electronic Industry Co., Ltd.; magnification ×6, working distance 39 mm) and connected to a video-recorder.

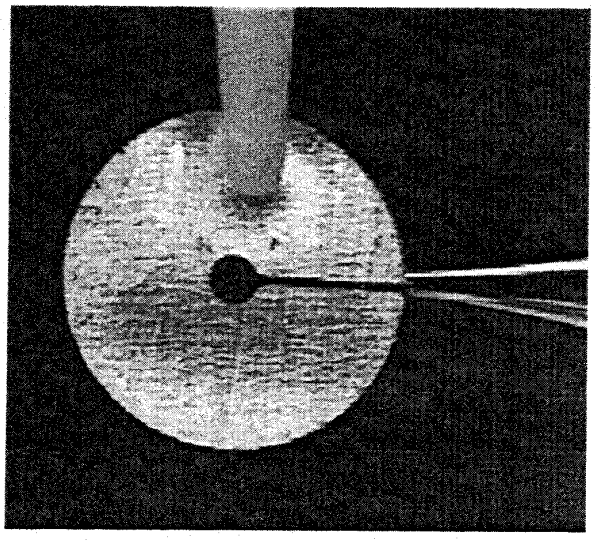

Fig. 1. Photograph of a disc-shaped film holder (the bright circular area) captured between the ceramic tips of tweezers. The central hole (the dark circle in the center of the holder), where the film is formed, is connected by a slit (the dark horizontal stripe) with the periphery of the holder. The tip of the glass capillary, used for formation of the liquid film, is seen to touch the outer end of the slit. The diameter of the film holder is 3 mm and the diameter of the central hole is 400 μm.

During film formation and thinning the film holder is fixed by tweezers of ceramic tips (attached to a rapid plunging device – a guillotine) inside a cylindrical isolating cell of diameter 4 cm and height 3

cm (see Fig. 3). The cell is made of transparent plastic material (polymethylmetacrylate) and has four orifices – two in the top and bottom walls (5 mm in diameter) for the tweezers, and two in the vertical wall (3 mm in diameter) for the glass capillary and for the camera observation. The bottom of the plastic cell is covered by aqueous layer, about 2 mm deep, which is warmed by heater. In this way the relative humidity inside the cell can be controlled to some extend and the water evaporation from the film is strongly suppressed. The experimental cell is isolated from the cryogen liquid (1 : 1 liquid mixture of ethane and propane at −190°C) by plastic sheet which is removed just before the film vitrification.

We use the following procedure for film formation. The holder is first captured by the tweezers and dipped into the working suspension. Alternatively, a drop of the suspension can be placed in the film holder by pipette. Some amount of the suspension fills up the central hole and the channel of the holder. Then the tweezers are attached to the guillotine, so the film holder is placed inside the isolating cell (Fig. 3). The glass capillary (partially pre-loaded with suspension) is adjusted by means of a *x-y-z*-micrometric screw to touch the external end of the channel. Gentle suction of liquid from the holder leads to the formation of a film, whose initial thickness is around a micrometer. Initially, the film spontaneously and rapidly (for a few seconds) thins down to ~ 100 nm, due to the sucking capillary pressure created by the concave shape of the meniscus surrounding the film (see, e.g., Refs. [37,38]). At a smaller thickness, the rate of film thinning decreases and, finally, either a stable equilibrium film is formed (if repulsive forces between the two film surfaces counterbalance the sucking capillary pressure) or the film ruptures at a certain critical thickness (typically, below 50 nm).

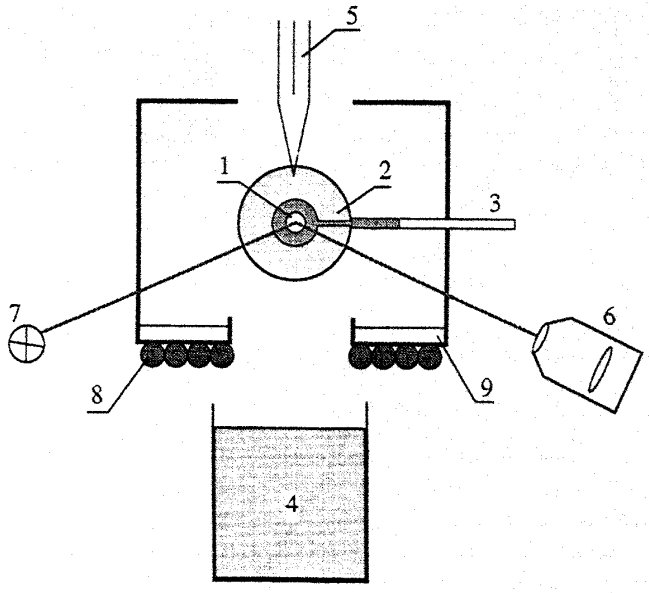

Fig. 3. Scheme of the experimental set-up. A liquid film (the thinnest planar portion of the suspension layer) (1) is formed in a disc-shaped film holder, (2) by gentle suction of a liquid through a glass capillary (3) that is connected to a microsyringe. When a film of required radius and thickness is obtained, it is plunged for vitrification into a cooling liquid (4) by means of a rapidly falling guillotine (5). The liquid film is monitored by a CCD-camera (6) in reflected monochromatic light (7). To control the water evaporation from the film we have to adjust the relative humidity of the air inside the experimental cell. For that purpose a heater (8) and a water pool (9) are used.

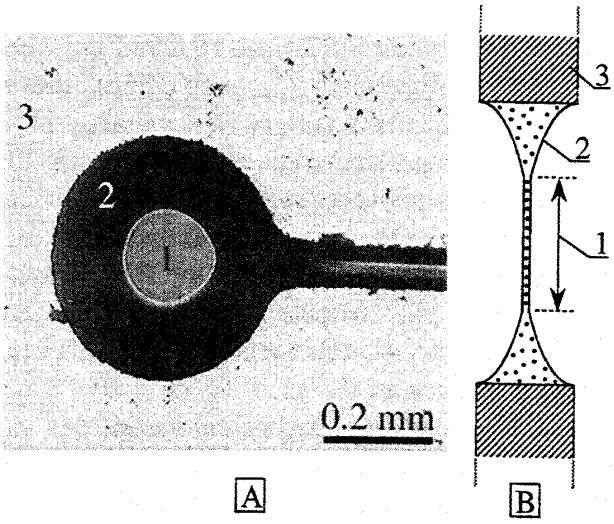

Fig. 2. (A) Photograph of a freely-suspended liquid film, formed in the central hole of the film holder. In reflected light the film (1) appears as a bright circular area (in the centre) surrounded by very dark meniscus region (2). The central part of the film holder (3) and a portion of the channel, connecting the meniscus with the glass capillary are also seen. (B) Schematic cross-section of the central part of the film holder (3) with the meniscus (2) and film (1) regions.

One should note that the film behaviour strongly depends on the composition and concentration of the suspension and can be very different for different samples. The processes of liquid film drainage and rupture are widely studied in colloid science due to their importance for the stability of disperse systems

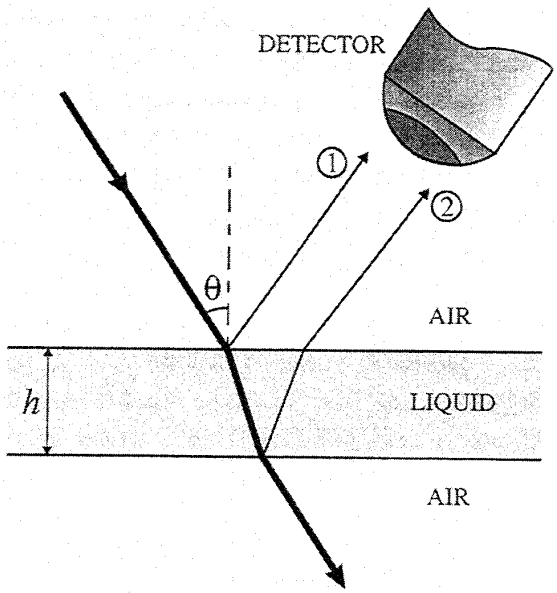

Fig. 4. Reflection of light from a thin liquid film. The incident beam is reflected from the two film surfaces. In general, the reflected beams, 1 and 2, are not in phase and interfere with each other. The intensity of the light captured by the detector, depends on the difference in the optical paths of the beams, i.e. on the film thickness, h, the refractive index of the liquid, n, and on the angle of incidence of the illuminating beam, θ [42].

(foams, emulsions, dispersions). Among the numerous literature on the liquid film stability one can refer to Refs. [37–41].

2.2. Film thickness determination

The reflection of light from an interface is described by Fresnel's low, which implies that the light intensity depends on the refractive indexes of the two phases and on the angle of incidence of the illuminating beam [42]. The reflection from a thin dielectric layer (film) is a more complex phenomenon, because the light meets two interfaces (Fig. 4). In the latter case the detector (e.g., eye, photomultiplier or CCD-camera) registers a pattern, resulting from the interference of light beams, reflected from the two film surfaces. With the film thinning process the reflected light intensity acquires several consecutive minima and maxima, corresponding to the condition for a negative or for a positive interference of the beams, respectively. The condition for interference is related to the optical path difference of the two beams [42], i.e. to the film thickness. This fact is used in the "microinterferometric" method [37] in which the film thickness is calculated from the intensity of the reflected light. For a perpendicular incident beam (with respect to the film plane) the film thickness, h, is given by the expression [37]

$$h = \left(\frac{\lambda}{4n}\right)\arcsin\left\{\frac{\Delta}{1+(1-\Delta)\left[4R/(1-R)^2\right]}\right\}^{1/2},$$

$$h \le \lambda/(4n), \qquad (1)$$

where λ is the light wavelength, n is the refractive index of the film substance, $R = (n-1)^2/(n+1)^2$, and

$$\Delta = \left(\frac{I - I_{\mathrm{MIN}}}{I_{\mathrm{MAX}} - I_{\mathrm{MIN}}}\right). \qquad (2)$$

Here I is the instantaneous value of the reflected light intensity, whereas I_{MAX} corresponds to the last interference maximum and I_{MIN} is the background. Major advantages of this method are: (i) only relative values of the light intensity are needed, and (ii) it is very accurate – typically, ± 1 nm in the film thickness range between 10 nm and 95 nm. Recent technical modifications of the method are described by Nikolov and Wasan [43] and Bergeron and Radke [44].

In previous studies [37,43,44] the reflected light intensities, I, I_{MAX} and I_{MIN}, were measured by fibre-optic probe, inserted in the eye-piece of an optical microscope, and connected to a photomultiplier. The incident and reflected beams were directed perpendicularly to the film surfaces by means of a semi-permeable mirror (for details see Refs. [43,44]). The photomultiplier output, as a function of time, was recorded by x–t chart-recorder and afterwards processed to calculate h.

We use a modified experimental set-up. The incident beam is taken from a standard illuminating unit (LA-30, Hayashi Co., Japan) and directed by an optical fibre toward the liquid film at an angle of incidence (θ in Fig. 4) equal to 6°. A dielectric optical filter, transparent to red light ($\lambda = 600 \pm 9$ nm), is placed on the optical path of the light to create a monochromatic incident beam. The non-zero angle of incidence, used in our set-up, leads to a small overestimation of the film thickness, as calcu-

lated from Eq. (1). By using more general expressions, presented in Chapter 2 of Ref. [42], we found that the resulting systematic inaccuracy in the calculated values of h is less than 0.3%, which is in the framework of the random experimental error and can be entirely neglected for our purpose. An important advantage of our optical system is the substantially improved contrast of the image, because the dispensing with semi-permeable mirror leads to a manifold reduction of the background intensity.

Another difference in our experiments is that instead of measuring the reflected light intensity by means of a photomultiplier, we applied an image analysis of the video-records of the film thinning process. The CCD-camera internal switch must be set to a "constant sensitivity mode" for such measurements. Digitised images of the film, in different moments of its thinning, are taken from the video-record by means of the program *Monitor* (Apple Computers) at the following values of the control parameters: Brightness = 0, Sharpness = 50, Saturation = 50, Hue = 50. Then the intensity of the reflected light is measured (in arbitrary units, a.u.) from the digitised images by using *Photoshop*™ (Adobe) program. The average intensity of a central region in the film, of size about a half of the film diameter, is typically measured. The power of the illuminating unit is pre-adjusted to ensure an intensity of the reflected light between 20 a.u. (the background) and 200 a.u. (I_{MAX}), whereas the saturation level of the *Photoshop* program is 235 a.u.

To check the linearity of the used CCD-camera and of the video-recording system, we performed a series of measurements with a set of neutral light filters of different transmittance. The latter was premeasured by means of a UV-visible spectrophotometer (UV-240, Shimadzu) at the working light wavelength (600 nm). Then the decrease in the intensity of a light beam, passing through the optical filters, was measured by using a CCD-camera, a video-recorder and an image analysis software, just like in the experiments with liquid films. The black circles in Fig. 5 show the data from the image analysis, plotted as a function of the filter transmittance, measured by the spectrophotometer. The straight line is obtained by means of the least-squares method and has a slope 0.997, and a correlation coefficient 0.9998. This result means, that the response of the video-system is linear in the whole range of measured intensities, which is a necessary condition for correct calculation of the film thickness by Eq. (1).

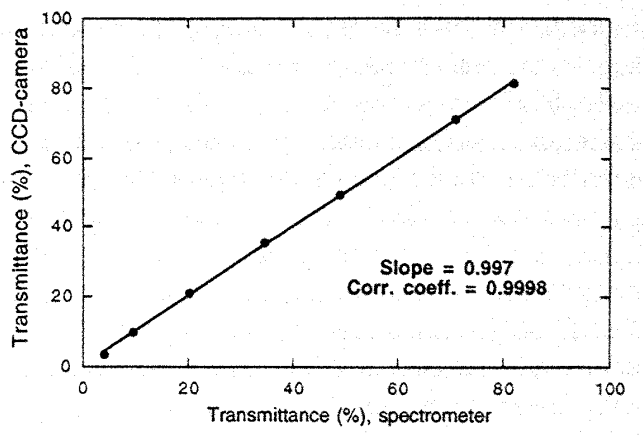

Fig. 5. Plot of the transmittance of neutral light filters measured by two different methods: (1) by a spectrophotometer (the abscissa), and (2) by a video-recording system and an image analysis software, used for the film thickness determination (the ordinate). The points are experimental data and the straight line is calculated by the least-squares method. The slope (0.997) and the correlation coefficient (0.9998) of the line show that the video-recording system has a linear response in the whole range of light intensities used in the film thickness measurements.

One should note that a certain random error in the film thickness determination is created by the experimental inaccuracy in measuring the exact values of I, I_{MAX}, and I_{MIN} (usually, this is the main source of inaccuracy in the microinterferometric method). We determined I_{MIN} from a video-record of an empty film holder (before placing the liquid drop in the holder), and I_{MAX} from the last interference maximum when the film is brightest (it corresponds to a film thickness $h = \lambda/4n = 112.8$ nm). At least 5 images were separately analysed for determination of I_{MAX} and I_{MIN}, respectively. The average value was taken for I_{MIN}, while the maximum measured value for I_{MAX} was used in the thickness calculations. Typically, the reproducibility in the value of I_{MIN} was about ± 0.5 a.u. and in the value of I_{MAX} – about ± 1 a.u. In some cases the liquid film was not perfectly flat at a large thickness and I_{MAX} was determined from the brightest film area.

The microinterferometric method implies that the film presents a homogeneous dielectric layer of refractive index, n, equal to the refractive index of the bulk suspension (e.g., $n \approx 1.33$ for aqueous suspensions). One should note that this assumption must be

applied with care to films containing particles of high concentration and of refractive index substantially different from that of the liquid. In such cases the mean particle concentration within the film could be different from the concentration in the bulk suspension [40]. Moreover, the effective film refractive index, n, could vary during the film thinning, which would cause an additional systematic error in the film thickness determination. That is why, the error in the film thickness determination could be substantially larger (several nanometers and even more) than that at optimal conditions (less than 1 nm) when films from very concentrated suspensions are studied.

2.3. Vitrification, transfer to the electron microscope and observation

When the liquid film attains its desired thickness and radius, the glass capillary is detached from the film holder, and the film is plunged for vitrification into 1 : 1 liquid mixture of ethane and propane, cooled by liquid nitrogen. We find this mixture particularly convenient for our experiment, because its freezing temperature is below the boiling point of the nitrogen, −196°C, although the pure ethane and propane are solid at this temperature (m.p. −183°C and −187.5°C, respectively). In this way we avoid the necessity of a special equipment for maintaining the liquid state of the cryogen. As known, the liquid ethane and propane are rather effective cryogens, because they possess very high cooling efficiency [45].

The vitrified films are transferred into the electron microscope by means of a cryo-transfer holder CT3500 (Oxford, UK). The cryo-holder and the cryo-transfer station are fed with dry nitrogen gas to prevent the frost accumulation over the sample (CT3500 Operator Manual, Oxford). One should note that the large vitrified films are rather fragile and any mechanical stress in direction perpendicular to the film surface easily brakes them. Therefore, the safe transfer of the frozen films onto the tip of the cryo-holder is often the most difficult (and fatal) step in our experiments.

The observations were performed at −190°C in JEM-1200 EX (JEOL, Japan) transmission electron microscope equipped with anticontaminator (JEOL). The accelerating voltage was 120 kV. The electron micrographs were taken with the minimum dose system to reduce the radiation damage and highly sensitive negative films (MEM, Mitsubishi Paper Mills, Ltd., Japan) were used. The shielding blades of the cryo-holder were opened at least 15 min after the insertion of the sample in the microscope to reduce the ice condensation on the specimen [46,47].

2.4. Array formation

The procedure for film control, described in Section 2.1, can be utilized to produce an ordered two-dimensional (2D) array of monodisperse particles in the liquid film, just before vitrification.

Direct observations by optical microscope [48] showed that polystyrene latex spheres of micrometer size could be ordered within an wetting film (a liquid film on a solid substrate) under the action of long-range, non-specific interactions. Initially, a relatively small in diameter wetting film was formed. When the film thickness became close to (or smaller than) the particle diameter, ordered 2D-clusters were formed under the action of an attractive interparticle capillary force, created by the deformation of the film surface around the particles [49,50]. Afterwards, the ordered clusters continuously grew in size as a result of a directional particle motion from the surrounding meniscus region towards the film. The film diameter must be gradually increased during this process, so that the boundary of the ordered particle monolayer to coincide with the transition zone planar film-meniscus. This stage of array growth was caused by the water evaporation from the film, which brings about a water influx from the surrounding meniscus toward the film [48]. In fact, this water influx (that compensates the water evaporated from the film) drags the suspended particles toward the ordered array in the planar film – see Fig. 6 (details are given in Refs. [48–50]).

One should note that in Refs. [48–50] the particles were usually considered to be partially hydrophobic (finite three-phase contact angle particle–water–air) as it is expected for polystyrene latex beads [51]. However, the mechanism and the consideration are similar in the case of hydrophilic particles

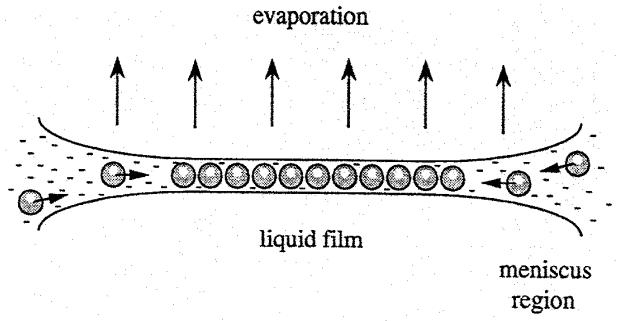

Fig. 6. Schematic presentation of the process of particle ordering in liquid films. A flux of particles, directed from the meniscus toward the film, appears as a result of the water evaporation from the film region. Details are given elsewhere [48,50].

(three-phase contact angle equal to zero) which are entirely immersed within the liquid film.

The same concept is used in the present study to obtain ordered arrays of nanometer sized particles in unsupported films. Initially, a small in diameter film is formed (~ 30 μm) and then gradually expanded up to 100–150 μm. At an appropriate particle concentration in the bulk suspension (about 10 vol%), a film expansion rate (5–10 μm/s), and a water evaporation rate, an ordered particle monolayer is formed within the film. A lower particle concentration and/or a rather fast film expansion lead to films deprived of particles and having thickness much smaller than the particle diameter. A higher particle concentration and an enhanced evaporation result in thick films containing bilayers (sometimes well ordered) and multilayers. The formation of a large in diameter film from the very beginning leads to disordered mono- or multilayers depending on the particle concentration. After getting some experience, one can easily distinguish these different states of the liquid film by considering the brightness of the film when observed in reflected light.

The mechanism, discussed above, implies that a liquid film of appropriate thickness (slightly larger than the particle diameter) serves as a two-dimensional matrix for the formation of an ordered monolayer of particles. Note that another physical mechanism can be also employed to order particles confined within a thin liquid film.

It has been recognised (see, e.g., Ref. [40]), that even a single planar surface can induce ordering among neighbouring particles if their concentration is high enough. The degree of the particle order increases even further, when the structured zones at two approaching surfaces overlap during a thin film formation [40,52,53]. As a result, the so called "oscillatory structural force" appears between the two film surfaces [40,54–56]. The action of the oscillatory structural force manifests itself in a stepwise decrease of the thickness of foam films containing particles of high concentration [43,44,57,58]. A semi-empirical formula, relating the height of the "steps" to the particle volume fraction, was proposed and compared with results from exact numerical calculations [54]. The observed multiple step-wise decrease of the film thickness is attributed to the layer-by-layer thinning of a particulate structure within the film [57]. This phenomenon is called "stratification" [43,44,57,58]. The freezing of a stratifying foam film (formed in the copper holder, Fig. 1) can be executed at each chosen stage of the film thinning process. Thus, a vitrified film containing a desired number of particle layers can be obtained and examined by cryo-electron microscopy [36]. In principle, the method is applicable to the study of particles of wide range of sizes (from nanometers to micrometers), which give rise to stratification, and especially to surfactant micelles, as demonstrated in Ref. [36].

Therefore, the stratification observed in our experiments with films containing surfactant micelles, latex spheres or bacteriorhodopsin vesicles, is related to some ordering of the particles within the liquid film. The results presented below and in Ref. [36] suggest that the larger particles form well ordered, colloid-crystal like structures, while the smaller particles (e.g., surfactant micelles) are less ordered.

In conclusion, two mechanisms of particle ordering in liquid films are possible: (i) through *directional particle flux, caused by the water evaporation from the film*, and (ii) a *surface induced ordering* when the film is formed from concentrated suspensions. In fact, both mechanisms are often simultaneously operative in our experiments (especially, when ordered multilayers are obtained). The directional flux leads to the accumulation of particles within the film (so, the particle concentration in the film is substantially higher, compared to the concentration in the bulk), which in turn leads to a surface induced ordering of the particles.

3. Illustrative results and discussion

The method for a specimen preparation, described above, can be applied to a variety of samples – we took micrographs of rotavirus, protein molecules, lipid vesicles and micelles. In comparison with the bare grid method [8] the main advantage of the present method is the possibility for precise film thickness monitoring, whereas the main disadvantage is the more difficult procedure for obtaining intact films in the electron microscope – the control of the liquid film and the transfer of the vitrified film require certain skills and practice. In some cases, however, the present method could produce specimens, which seem at the present not attainable by the other cryo-methods for sample preparation. Several illustrative examples are presented and discussed below.

As mentioned in the Introduction, one of the main advantages of the cryo-electron microscopy is the possibility for investigation of macromolecules and molecular complexes that are unstable when dried. However, the contrast of ice-embedded specimens is relatively low, and an image averaging over many particles is required for high resolution structural analysis [1–4]. For that purpose, ordered two-dimensional arrays (or even two-dimensional crystals, if available) of particles are desirable [59]. A variety of methods for formation of two-dimensional (2D) crystals of membrane and water soluble proteins were developed [60], but ice embedded arrays of viruses or of other large protein complexes were observed only occasionally [1,61]. In the following subsections, 3.1 and 3.2, we demonstrate that two-dimensional arrays of spherically symmetrical particles can be reproducibly obtained by our procedure.

3.1. Ordered array of latex spheres

This set of experiments was performed to demonstrate that no specific attractive interactions are needed to obtain a particle array by the procedure described in Section 2.4. In Fig. 7 a vitrified film containing a well ordered monolayer of latex spheres (144 nm $\pm 1\%$ in diameter; SC-015-S, Stadex, Japan) is shown. The concentration of the latex particles in the bulk suspension was 8 vol%. Due to the convective particle flux driven by water evaporation (Fig.

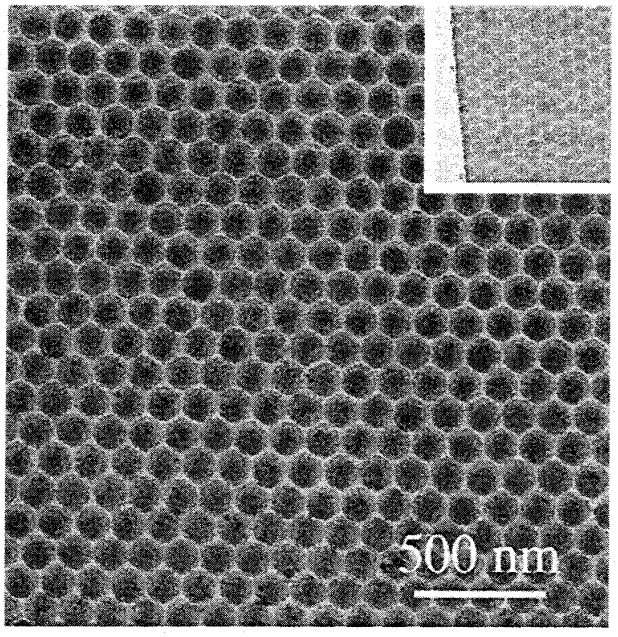

Fig. 7. Ordered monolayer of polystyrene latex spheres (144 nm in diameter) in a vitrified film of thickness close to the particle diameter. The inset shows the edge of a broken vitrified film – one sees that the crack passes through the latex particles and follows the direction of the array axis.

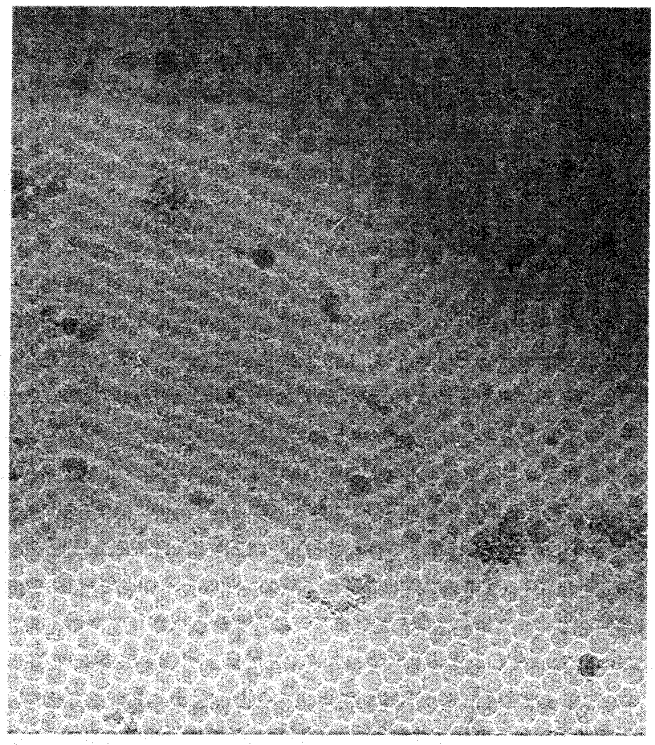

Fig. 8. Ordered monolayer (the brighter area at the bottom), bilayer (middle) and triple-layer (the darker top region) of latex spheres (144 nm in diameter) in a vitrified film. The randomly distributed darker spots are microscopic ice crystals deposited on the vitrified film as a contamination.

6), the particles accumulated in the film region and formed a dense, well ordered monolayer. At the periphery of the monolayer region we obtained bilayer, triple-layer and sometimes four-layer bands – see Fig. 8. The particles were ordered in these multilayers and different types of domains could be distinguished. We were able to control to some extent the area of the multilayers by varying the film expansion rate. A slower increase of the film radius resulted in larger bi- and triple-layer regions at the expense of the monolayer. Similar results were obtained with a smaller in size latex (66 nm in diameter, C-101.1, IDC, Oregon). However, the polydispersity of the smaller particles was substantially larger ($\pm 7.3\%$) and the formed 2D-array was distorted.

One should note that the vitrified ordered latex films were particularly fragile and it was very difficult (and rare) to transfer them intact into the electron microscope. The vitrified aqueous films were much more stable at a similar thickness. One possible explanation of this fact was suggested by the observation that the cracks formed in the latex film usually passed through the particles along one of the array axes – see the inset in Fig. 7. Probably, the polystyrene becomes very fragile at low temperature and the latex particles can be easily broken. A difference in the thermal expansion coefficients of polystyrene and water could additionally create an internal stress in the latex layer upon the vitrification and facilitate the film rupture.

As discussed in the previous section it is not possible to measure accurately the thickness of films containing latex particles of high concentration. The refractive index of the polystyrene latex spheres ($n = 1.56$) is substantially higher than that of water ($n = 1.33$). Therefore, the assumption that the film can be modelled as an uniform dielectric layer having a refractive index equal to that of the bulk suspension is strongly violated and Eq. (1) cannot be applied. That is why we do not know the exact film thickness, and whether the latex spheres are entirely or partially immersed in the aqueous layer, in these experiments.

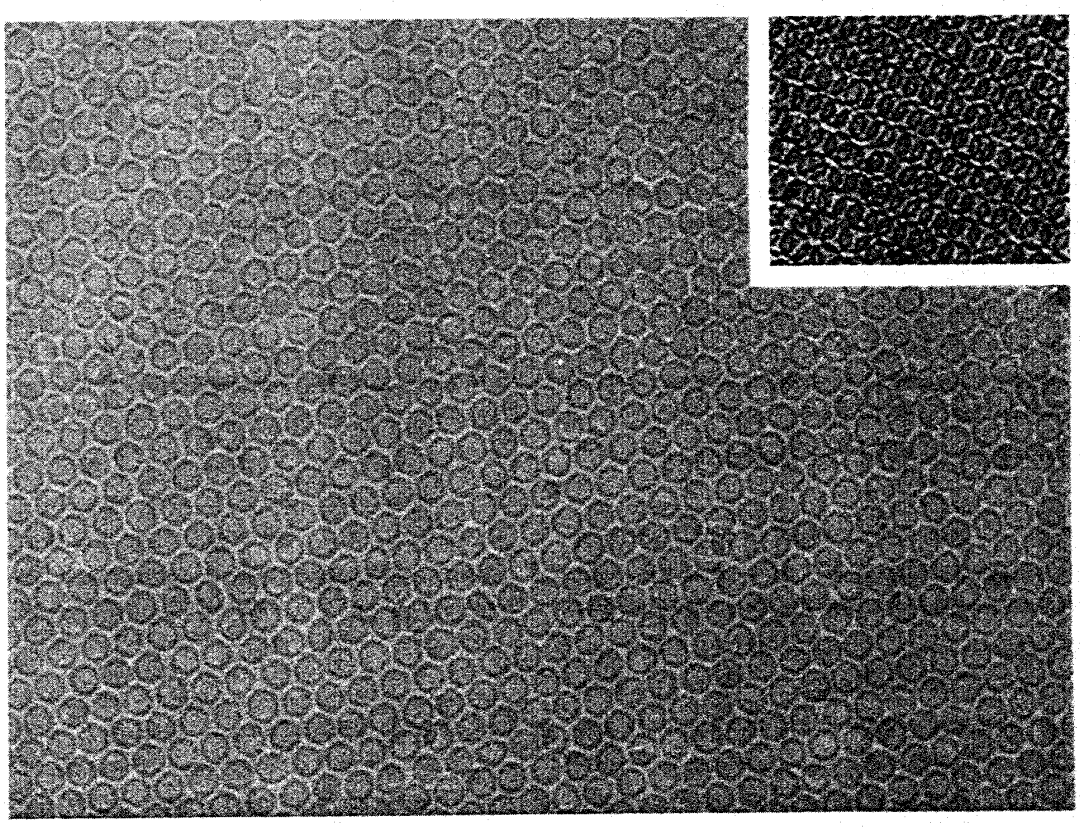

Fig. 9. Ordered monolayer of bacteriorhodopsin vesicles. The liquid film thickness was 59 nm just before vitrification. The mean interparticle center-to-center distance is 44.7 nm. The inset shows an ordered bilayer of vesicles.

3.2. Ordered array of bacteriorhodopsin vesicles

This sample contains spherical vesicles made of the membrane protein bacteriorhodopsin (bR) – see Kouyama et al. [62]. The bR vesicles are photoactive (like the purple membrane of *Halobacterium Halobium* from which they are produced) but the mechanism of their formation and details in the vesicle structure are still not available. The structure of these "soft" vesicles cannot be investigated by the negative staining method because they are easily deformed or even totally destroyed by the staining reagents (unpublished data). Therefore, the cryo-microscopy seems an appropriate tool for investigating these particles.

In Fig. 9 we show a photograph of an ordered vitrified monolayer of bR vesicles obtained as described above. Such ordered array is produced only at a film thickness slightly above the vesicle diameter ($h = 59$ nm in this case) and under a precise control of the film expansion process. The quality of the long-range order is very good – thousands of particles could be grouped within a single domain. We found, however, that the vesicles are slightly polydisperse (i.e. the particles are not identical). The mean diameter measured from digitised images is 38.8 nm with standard deviation of ± 2.2 nm. The mean centre-to-centre distance is 44.7 nm. Structural analysis, including averaging over similar in size and orientation particles, is under a way and will be presented in a separate study. The inset in Fig. 9 shows an ordered bilayer of bR-vesicles. In the same vitrified film we observed regions containing three and four layers of vesicles.

4. Conclusions and prospect for future work

A novel method for preparation of unsupported vitrified films for cryomicroscopy is described. The main features of the method are the possibilities for liquid film observation and control before freezing. These allow a precise measurement of the liquid film thickness and a choice of an appropriate moment for film vitrification. In addition, the method provides the possibility for production of ordered particle arrays in the liquid film just before freezing. As an illustration, ordered mono- and multilayers of latex microspheres and bacteriorhodopsin vesicles are obtained.

The most severe limitation of the method seems to be the minimal thickness of the film, which can be transferred intact into the electron microscope. With our procedure we transferred reproducibly (probability close to 30%) films of thickness around 50 nm and above. In several experiments we succeeded to transfer intact films of thickness 27–30 nm [36]. We expect that an automatic device for setting the film holder in the cryo-holder tip could substantially overcome this problem and the observation of films as thin as 20 nm will become attainable. A system for environmental control, like that developed by Bellare et al. [63], could be helpful in many cases.

The present method can be useful in several areas. For example, systems composed of colloid particles (micelles, proteins, microemulsion droplets, vesicles, latex spheres) could be studied. The mutual relationship between the film thickness and stability on one side, and the particle structure and arrangement, on the other side, can be quantitatively investigated. A revealing the factors, which affect and control the stability of liquid films, is a very important problem from fundamental viewpoint, as well as for the industrial application of dispersions.

Large in area, homogeneous vitrified films of known thickness can be used for the investigation of the electron scattering cross-section [64] of vitrified water and aqueous solutions.

In structural biology, the method could be applied to viruses, vesicles, ribosomes, etc. It provides the advantage to be able to select the most suitable film thickness for vitrification in order to ensure the best contrast and the absence of "flattening" effect [1]. Vitrified two dimensional crystalline or paracrystalline arrays of viruses might allow a high resolution structural analysis. The method can be further developed, e.g., by combining the film control with some of the established techniques for protein crystallisation at a single air–water interface [60,65,66].

Acknowledgements

This work was performed under the program Exploratory Research for Advanced Technology (ERATO, JRDC). The bacteriorhodopsin vesicles

were kindly supplied by Dr. T. Kouyama (RIKEN, Saitama, Japan). The critical reading of the manuscript by Professor P.A. Kralchevsky (University of Sofia, Bulgaria), and the useful discussions with him, Dr. T. Scheybani (Max-Planck-Institute fur Biochemie, Martinsried, Germany) and Dr. O.D. Velev (University of Sofia, Bulgaria) are gratefully acknowledged. The authors are grateful to Dr. T. Miwa (Protein Array Project, ERATO, JRDC, Japan) for his help in computers.

References

[1] J. Dubochet, M. Adrian, J.-J. Chang, J.-C. Homo, J. Lepault, A.W. McDowall and P. Schultz, Quart. Rev. Biophys. 21 (1988) 129.
[2] W. Chiu, Annu. Rev. Biophys. Biomol. Struct. 22 (1993) 233.
[3] K.A. Taylor and R.M. Glaeser, J. Ultrastructure Res. 55 (1976) 448.
[4] R.A. Milligan, A. Brisson and P.N.T. Unwin, Ultramicroscopy 13 (1984) 1.
[5] International Experimental Study Group, J. Microscopy 141 (1986) 385.
[6] Y. Talmon, M. Adrian and J. Dubochet, J. Microscopy 141 (1986) 375.
[7] P. Echlin, J. Microscopy 161 (1991) 159.
[8] M. Adrian, J. Dubochet, J. Lepault and A.W. McDowall, Nature 308 (1984) 32.
[9] J. Lepault and K. Leonard, J. Mol. Biol. 182 (1985) 431.
[10] R.H. Vogel, S.W. Provencher, C.H. von Bonsdorff, M. Adrian and J. Dubochet, Nature 320 (1986) 533.
[11] S.D. Fuller, Cell 48 (1987) 923.
[12] Y. Fujiyoshi, N.P. Kume, K. Sakata and S.B. Sato, EMBO J. 13 (1994) 318.
[13] R. Henderson and P.N.T. Unwin, Nature 257 (1975) 29; P.N.T. Unwin and R. Henderson, J. Mol. Biol. 94 (1975) 425.
[14] R. Henderson, J.M. Baldwin, T.A. Ceska, F. Zemlin, E. Beckmann and K.H. Downing, J. Mol. Biol. 213 (1990) 899.
[15] W. Kühlbrandt, D.G. Wang and Y. Fujiyoshi, Nature 367 (1994) 614.
[16] W. Kühlbrandt, Curr. Opinion Struct. Biol. 4 (1994) 519.
[17] P.N.T. Unwin, Nature 373 (1995) 37.
[18] E.M. Mandelkow, R. Rapp and E. Mandelkow, J. Mol. Biol. 181 (1985) 123; J. Microscopy 141 (1986) 361.
[19] J. Trinick, J. Cooper, J. Seymour and E.H. Egelman, J. Microscopy 141 (1986) 349.
[20] E.P. Gogol, U. Lucken, T. Bork and R.A. Capaldi, Biochemistry 28 (1989) 4709.
[21] E.P. Gogol, R. Aggeler, M. Sagermann and R.A. Capaldi, Biochemistry 28 (1989) 4717.
[22] G. Mosser, V. Mallouh and A. Brisson, J. Mol. Biol. 226 (1992) 23.
[23] J. Lepault, F. Pattus and N. Martin, Biochim. Biophys. Acta 820 (1985) 315.
[24] P.M. Frederik, M.C.A. Stuart, P.H.H. Bomans, W.M. Busing, K.N.J. Burger and A.J. Verkleij, J. Microscopy 153 (1988) 81; 161 (1991) 253.
[25] K. Sakata, Y. Tahara, K. Morikawa, Y. Fujiyoshi and Y. Kimura, Ultramicroscopy 45 (1992) 253.
[26] Y. Tahara and Y. Fujiyoshi, Micron 25 (1994) 141.
[27] S. Chiruvolu, S. Walker, J. Israelachvili, F.-J. Schmitt, D. Leckband and J.A. Zasadzinski, Science 264 (1994) 1753.
[28] J. Dubochet, M. Adrian, J. Teixeira, C.M. Alba, R.K. Kadiyala, D.R. MacFarlane and C.A. Angell, J. Phys. Chem. 88 (1984) 6727.
[29] J.R. Bellare, T. Kaneko and D.F. Evans, Langmuir 4 (1988) 1066.
[30] P.K. Vinson, J.R. Bellare, H.T. Davis, W.G. Miller and L.E. Scriven, J. Colloid Interface Sci. 142 (1991) 74.
[31] O. Regev, C. Kang and A. Khan, J. Phys. Chem. 98 (1994) 6619.
[32] Z. Lin, R.M. Hill, H.T. Davis, L.E. Scriven and Y. Talmon, Langmuir 10 (1994) 1008.
[33] A. Knoblich, M. Matsumoto, K. Murata and Y. Fujiyoshi, Langmuir 11 (1995) 2361.
[34] J. Dubochet, J. Lepault, R. Freeman, J.A. Berriman and J.C. Homo, J. Microscopy 128 (1982) 219.
[35] U. Jakubowski and M. Mende, J. Microscopy 161 (1991) 241.
[36] N.D. Denkov, H. Yoshimura, K. Nagayama and T. Kouyama, Phys. Rev. Lett. 76 (1996) 2354.
[37] A. Scheludko, Adv. Colloid Interface Sci. 1 (1967) 391.
[38] I.B. Ivanov, Ed., Thin Liquid Films: Fundamentals and Applications (Dekker, New York, 1988).
[39] B.V. Derjaguin, N.V. Churaev and V.M. Muller, Surface Forces (Consultants Bureau, Plenum, New York, 1987).
[40] J. Israelachvili, Intermolecular and Surface Forces (Academic Press, London, 1992).
[41] V.N. Izmailova, G.P. Yampol'skaia and B.D. Summ, Surface Phenomena in Protein Systems (Chimia, Moscow, 1988) [in Russian].
[42] M. Born and E. Wolf, Principles of Optics, 6th ed. (Pergamon, Oxford, 1980).
[43] A.D. Nikolov and D.T. Wasan, J. Colloid Interface Sci. 133 (1989) 1.
[44] V. Bergeron and C.J. Radke, Langmuir 8 (1992) 3020.
[45] S.M. Bailey and A.N. Zasadzinski, J. Microscopy 163 (1991) 307.
[46] J.-C. Homo, F. Booy, P. Labouesse, J. Lepault and J. Dubochet, J. Microscopy 136 (1984) 337.
[47] P.M. Frederik and W.M. Busing, J. Microscopy 144 (1986) 215.
[48] N.D. Denkov, O.D. Velev, P.A. Kralchevsky, I.B. Ivanov, H. Yoshimura and K. Nagayama, Langmuir 8 (1992) 3183; Nature 361 (1993) 26.
[49] P.A. Kralchevsky, V.N. Paunov, N.D. Denkov, I.B. Ivanov and K. Nagayama, J. Colloid Interface Sci. 155 (1993) 420.

[50] P.A. Kralchevsky, N.D. Denkov, V.N. Paunov, O.D. Velev, I.B. Ivanov, H. Yoshimura and K. Nagayama, J. Phys.: Condens. Matter 6 (1994) A395.
[51] A. Hadjiiski, R. Dimova, N.D. Denkov, I.B. Ivanov and R. Borwankar, Langmuir (1996) in press.
[52] J.E. Hug, F. van Swol and C.F. Zukoski, Langmuir 11 (1995) 111.
[53] X.L. Chu, A.D. Nikolov and D.T. Wasan, Langmuir 10 (1994) 4403.
[54] P.A. Kralchevsky and N.D. Denkov, Chem. Phys. Lett. 240 (1995) 385; Prog. Colloid Polymer Sci. 98 (1995) 18.
[55] P.A. Kralchevsky, K.D. Danov and N.D. Denkov, Chemical Physics of Colloid Systems and Interfaces, in: Handbook of Surface and Colloid Chemistry, Ed. K.S. Birdi (CRC Press, London, 1996).
[56] M.L. Pollard and C.J. Radke, J. Chem. Phys. 101 (1994) 6979.
[57] A.D. Nikolov, P.A. Kralchevsky, I.B. Ivanov and D.T. Wasan, J. Colloid Interface Sci. 133 (1989) 13.
[58] A.D. Nikolov, D.T. Wasan, N.D. Denkov, P.A. Kralchevsky and I.B. Ivanov, Prog. Colloid Polymer Sci. 82 (1990) 87.
[59] L.A. Amos, R. Henderson, P.N.T. Unwin, Prog. Biophys. Mol. Biol. 39 (1982) 183.
[60] B.K. Jap, M. Zulauf, T. Scheybani, A. Hefti, W. Baumeister, U. Aebi and A. Engel, Ultramicroscopy 46 (1992) 45.
[61] B. Alberts, D. Bray, J. Lewis, M. Raff, K. Roberts and J.D. Watson, Molecular Biology of the Cell, 3rd ed. (Garland, London, 1994) Fig. 4-30.
[62] T. Kouyama, M. Yamamoto, N. Kamiya, H. Iwasaki, T. Ueki and I. Sakurai, J. Mol. Biol. 236 (1994) 990.
[63] J.R. Bellare, H.T. Davis, L.E. Scriven and Y. Talmon, J. Electron Microsc. Tech. 10 (1988) 87.
[64] R. Eusemann, H. Rose and J. Dubochet, J. Microscopy 128 (1982) 239.
[65] R.D. Kornberg and S.A. Darst, Curr. Opinion Struct. Biol. 1 (1991) 642.
[66] A. Brisson, A. Olofsson, P. Ringler, M. Schmutz and S. Stoylova, Biol. Cell 80 (1994) 221.